DOI: 10.1070/RCR4652

Photochromic magnetic materials based on transition metal oxalate complexes †

Sergey M. Aldoshin, Nataliya A. Sanina

Institute of Problems of Chemical Physics, Russian Academy of Sciences
prosp. Akademika Semenova 1, 142432 Chernogolovka, Moscow Region, Russian Federation

The review discusses theoretical and experimental approaches to the design of compounds which combine photochemically active groups and magnetic species in the same crystal lattice and can serve as the basis for the development of novel materials with specified properties and functions, including high-purity composites and nanomaterials. Data on the synthesis, structures and magnetic properties of para- and ferromagnetic 3d metal tris(oxalate) complexes with various organic photochromic cations are summarized. The assembly of the complexes to ordered nanostructures and polymer composites is considered.
The bibliography includes 62 references.

Contents

I. Introduction 1185
II. Design of bifunctional systems with magnetic 3d metal anions, bridging bidentate ligands and photochromic cations 1186
III. Synthesis, structures and properties of para- and ferromagnetic crystals with photochromic cations of the spirocyclic series 1189
IV. Synthesis and properties of materials based on photochromic 3d metal tris(oxalates) 1193

I. Introduction

The functionalization of molecular systems in order to impart two or more desired properties to new materials is currently one of the hot topics in chemistry and physics of new materials. A combination of different physical properties (superconductivity, magnetism, photochromism, nonlinear optical properties and so on) in the same crystal lattice and possible synergistic effects can give rise to new properties and lead to new applications in molecular electronics. The design of such compounds and related materials will enable the control of one of the properties by changing another property in response to external stimuli (temperature, light, magnetic and electric fields depending on the combination of the properties of the material). Such multifunctional materials can serve as the basis for the development of molecular spintronics. Despite the obvious progress in this field, the formulation of principles for the design of multifunctional materials, the optimization of their properties and the establishment of relevant structure – property relationships are still important issues to be addressed in molecular materials science.

Therefore, a challenge is the crystal-chemical design of materials which combine structural units responsible for photochromic and magnetic properties in the same crystal lattice. Photochromic systems are considered [1 – 3] as promising materials for optical data recording and storage devices,[4] optical switches,[5, 6] transistors,[7, 8] chemical sensors [9] and so on.

Strategic approaches to the photomodulation of magnetic properties in hybrid molecular systems possessing both the magnetic and optical properties were considered for the first time in reviews.[10, 11] Based on the analysis of experimental data, these approaches can be divided into two groups: 1) the influence of the photochromic sublattice on the bulk behaviour of molecule-based magnets and 2) the photocontrol of intra- and intermolecular magnetic coupling. The first approach is based on a combination of different types of light-sensitive and magnetic units in the same crystal lattice.[10, 11] The second approach relies on the creation of molecules containing fragments (or centres) with unpaired spins and photochromic fragments.

In the framework of the second approach, photoinduced charge-transfer phase transitions, changes in the spin state of magnetic centres, photoswitching of intramolecular exchange interactions between magnetic centres linked by

S.M.Aldoshin. Academician, Director of the IPCP RAS.
Telephone: +7(495)933 – 5707, e-mail: sma@icp.ac.ru
Current research interests: synthesis, structure and reactivity of organic compounds; solid-state chemistry; organic and functional hybrid materials; fundamental problems of the formation of new materials.
N.A.Sanina. Doctor of Chemical Sciences, Head of the Department of the Structure of Matter at the same Institute.
Telephone: +7(496)522 – 1168, e-mail: sanina@icp.ac.ru
Current research interests: synthesis and reactivity of organic and inorganic complex compounds.

Received 1 April 2016
Translation: T.N.Safonova

† Dedicated to Academician O.M.Nefedov on the occasion of his 85th birthday.

© 2016 Russian Academy of Sciences and Turpion Ltd.

a photochromic bridge, the generation of high-spin organic molecules that form high-spin groups through intermolecular exchange interactions, *etc.* are summarized in the mentioned reviews.[10,11] The development of these ideas and analysis of experimental data were later considered in a book.[12]

This review presents the analysis of theoretical and experimental data obtained during recent years in the framework of the first approach, including the design of new multifunctional hybrid compounds, which combine magnetic and photochromic sublattices in the same crystal lattice, and the creation of materials based on these compounds. The development of such materials (polymer composites and nanostructures) not only allows the combination of several functions in the same lattice, which is important for the reduction of the size of the element basis in modern devices, but also enables the control and variation of these properties through synergistic effects. The available results suggest that new materials suitable for various practical applications can be created by means of the crystal-chemical design.

II. Design of bifunctional systems with magnetic 3d metal anions, bridging bidentate ligands and photochromic cations

II.1. Magnetic sublattice

Transition metal coordination polymers with various ligands which have a layered or framework structure required for magnetism are well known.[13] Bimetallic tris(oxalate) complexes with the stoichiometry $Ct^+[M^{II}M^{III}(ox)_3]^-$ (M^{II} = V, Cr, Mn, Fe, Co, Ni, Cu, Zn; M^{III} = Cr, Fe; ox = $C_2O_4^{2-}$) were synthesized and investigated in detail. It was firmly established that the cations $Ct^+ = [R_4E]^+$ (E = N, P; R = Ph, Pr^n, Bu^n, n-C_5H_{11}) promote the formation of two-dimensional honeycomb layered structures as the solid phase. First data on the structures of bimetallic 3d metal tris(oxalates) of the composition $[R_4N][M^{II}M^{III}(ox)_3]$ (R = Bu^n, *etc.*; M^{II} = Mn, Fe, Co, Ni, Cu; M^{III} = Cr, Fe, Mn) were reported.[14–16]

Complexes with these anions have properties typical of ferro- (M^{III} = Cr) and ferrimagnets (M^{III} = Fe). The magnetic ordering is induced by exchange interactions between oxalate-bridged metal ions. The Curie temperature (T_C) and the parameters of the magnetic hysteresis loop are determined by both the size of the cation and the nature of metals. Thus, complexes of the series $[Bu^n_4N][M^{II}Cr^{III}(ox)_3]$ are transformed into a ferromagnetic state at $T_C < 14$ K [the maximum value corresponds to Ni^{II}; the minimum value (6 K), to Mn^{II}]. The complexes $[Bu^n_4N][M^{II}Fe^{III}(ox)_3]$ (M^{II} = Fe, Ni) exhibit ferromagnetic properties at temperatures <43 and 28 K, respectively. It was shown[17–20] that the crystal structures of the systems of this type are composed of bimetallic layers of hexagonal symmetry and bulky organic tetraalkylammonium cations that are located between these layers (Fig. 1). The replacement of a nonfunctional organic cation with a functional cation can be used to vary the properties of these magnets and create new hybrid molecular materials with interesting properties dependent on the nature of the cation. For example, the intercalation of the ferrocenium cation between the layers of the bimetallic network $[M^{II}M^{III}(ox)_3]_n$ (M^{III} = Cr, Fe; M^{II} = Mn, Fe, Co, Ni, Cu) gave compounds that combine

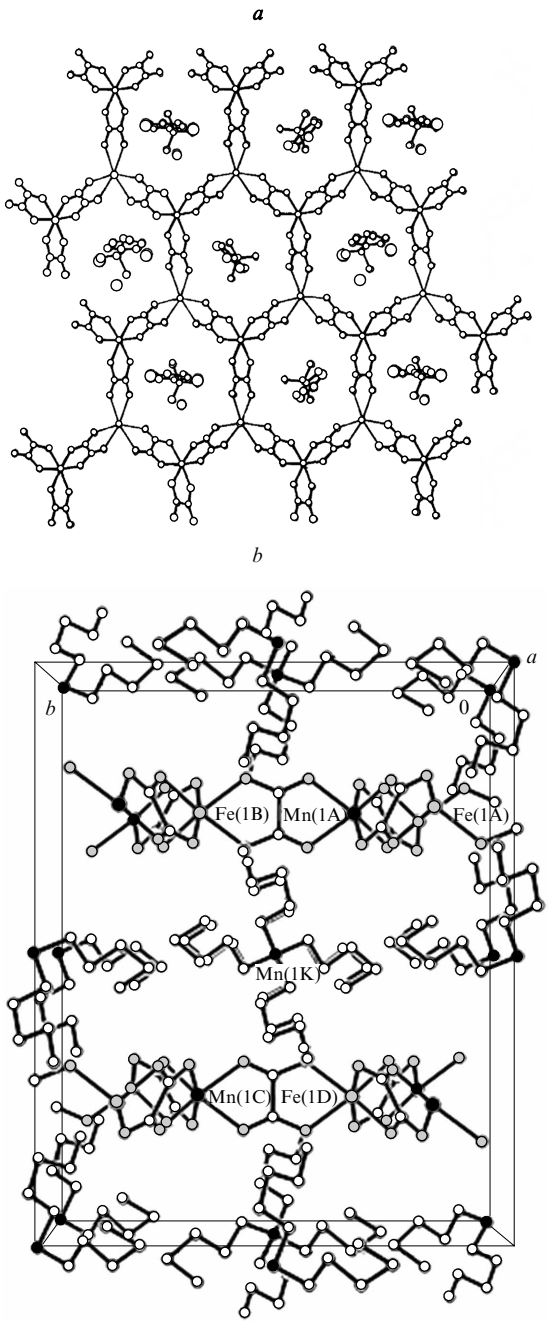


Figure 1. Fragment of the layer in the crystal structure of $[Bu^n_4N]^+[Fe^{III}Mn^{II}(ox)_3]$.[20]
(*a*) Side view, (*b*) top view.

either ferromagnetic (for M^{III} = Cr) or antiferromagnetic (for M^{III} = Fe) properties of the network and the paramagnetic properties of the decamethylferrocenium cation ($Cp^*_2Fe^+$).[21] Crystalline materials that combine both magnetism and conductivity[22,23] or have both magnetic and nonlinear optical properties[24,25] were prepared.

The search for bridging ligands and metal pairs providing the strongest metal–metal ferromagnetic exchange interactions in such anions is still an important problem. For example, due to the delocalized π-electron system, the planar chloranilate dianion ($ClAn^{2-}$) is of interest as a possible mediator for exchange interactions between

unpaired electrons of paramagnetic metal centres and can be considered as a promising ligand for the design of new molecule-based magnets. In the study,[26] the first method was proposed for the assembly of heterometallic coordination polymers with a two-dimensional honeycomb layered structure composed of octahedral fragments $[Fe(ClAn)_3]$ by using divalent 3d metals. The complex $[Bu^n_4N][MnFe(ClAn)_3]$ is the first compound with chloranilate bridging ligands that undergoes transitioni to an antiferromagnetic state at $T > 2$ K.

The authors of this review calculated the exchange coupling constants (J) and analyzed the spin density distribution in the complex anions $[L_2M^{1(III)}LM^{2(II)}L_2]^{n-}$, where L is a ligand [oxalate, oxamide (oxam), hydroxamate (HA), dithiooxamide (diSox)], M^1 and M^2 are trivalent and divalent 3d metals, respectively, and n is the charge of the anion,[27] at the B3LYP/TZV level of theory using the GAUSSIAN-03 program.[28] It was shown that the strongest exchange magnetic interaction of the required type in anion layers of the magnetic sublattice is achieved by a combination of particular metal pairs and bridging ligands. The calculations demonstrated that the complexes formed by $Cr^{III}-Ni^{II}$ or $Cr^{III}-Co^{II}$ pairs with dithiooxamide ligands should have the highest J values (Table 1).

The differences of the calculated constants J from the experimental values are within a few cm^{-1}. In these complexes, the spin density is located almost entirely at the metal atoms (Fig. 2): for the complexes containing the Cr–Ni pair, >95% of the spin density is located at the metal pair; for the complexes containing the Cr–Co pair, this value is >97%. As can be seen in Fig. 2, the spin density is almost absent at the atoms adjacent to the Cr atom, whereas in complexes with the Ni atom, the spin density is transferred to adjacent atoms.

Table 1. Spin populations [ρ(M)] at metal atoms in complexes containing Cr–Co or Cr–Ni pairs and a bridging ligand, total changes in the spin populations at the metal pair compared to their values for the isolated cations $\{[\Delta(\rho(M^1)+\Delta(\rho(M^2)]\}$ and the constants J.[27]

Parameter of the complex	Bridging ligand			
	diSox	oxam	ox	HA
	Pair Cr–Co			
ρ(Cr)	3.209	3.073	3.046	3.009
ρ(Co)	2.687	2.794	2.792	2.812
$[\Delta\rho(Cr)+\Delta\rho(Co)]$	0.522	0.279	0.254	0.197
J/cm^{-1}	8.92	7.01	5.09	3.13
	Pair Cr–Ni			
ρ(Cr)	3.210	3.074	3.045	3.008
ρ(Ni)	1.599	1.737	1.738	1.765
$[\Delta\rho(Cr)+\Delta\rho(Co)]$	0.611	0.337	0.307	0.243
J/cm^{-1}	14.42	10.29	8.32	5.54

Note. The constants J were calculated from the equation $J = -(E[HS]-E[BS])/(\langle S^2\rangle_{HS}-\langle S^2\rangle_{BS})$, where E is the total energy of the state, HS is the high-spin state, BS is the broken-symmetry state, and S is the total spin.[29] In the ORCA program, the exchange coupling constants are calculated using equations derived from the analysis of the spin-Hamiltonian $H = -2J\cdot S_A\cdot S_B$ (Heisenberg–Dirac–van Vleck model).

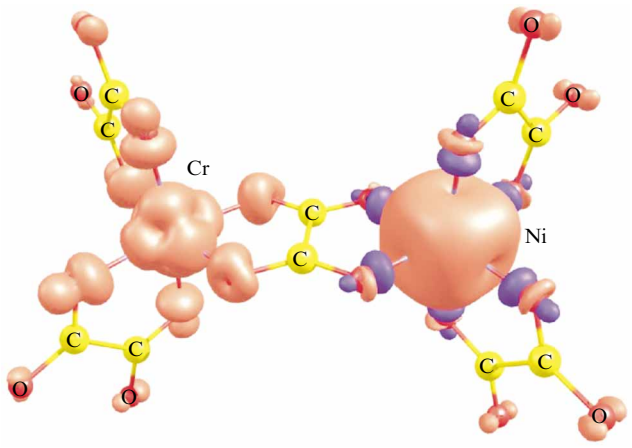


Figure 2. Spin density distribution in the complex anion $[(ox)_2Cr^{III}(ox)Ni^{II}(ox)_2]^{5-}$ exhibiting ferromagnetic exchange interactions.[27]

Investigations of the relationship between the exchange coupling constant and the spin density distribution in complexes that form a bimetallic network and the elucidation of the mechanism of exchange interactions in the complexes provide additional information required for the control of exchange interactions in the resulting magnetic sublattices.

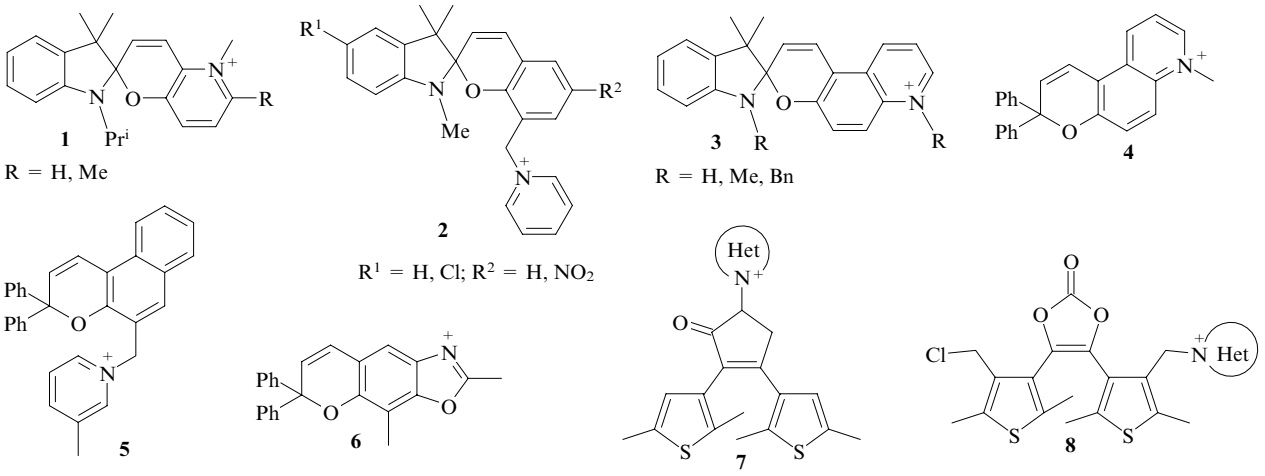
As can be seen in Table 1, there is a correlation in the changes in these values. Thus, an increase in the spin density transfer from Co^{II} to Cr^{III} is accompanied by an increase in the constant J, *i.e.*, the bridging ligand mediates the spin density transfer from one metal atom to another. The spin density is exchanged between the metal atoms. This fact provides deeper insight into the nature of exchange interactions in these complexes. The higher the degree of spin density transfer from one metal to another, the larger the exchange coupling constant between these atoms, *i.e.*, the magnetic properties become more pronounced with an increase in the degree of spin density redistribution. In turn, the degree of spin density transfer is apparently higher in the cases, when the direction of unpaired-electron orbitals coincides with the directions of the chemical bonds of the bridging ligand. This is the case with the Ni atom, as opposed to the Co atom, resulting in a higher degree of spin density transfer and larger values of J.

Therefore, the above-considered data can be used for the design of required magnetic sublattices of new multifunctional compounds.

II.2. Photochromic sublattice

Spiropyran halides SP^+X^- (for example, the salts with the SP^+ cations of types **1**–**3**), chromene halides Chr^+X^- (cations **4**–**6**) and diarylethene halides DAE^+X^- (cations **7** and **8**) hold considerable promise for preparing crystals of tris(oxalate) molecule-based magnets with photochromic organic cations. Therefore, the synthesis of these compounds and investigations of their structures and solid-state photoactivity have attracted our considerable attention.[30–37] The features responsible for reversible photochromic transformations of the cation sublattice of spiropyran under the crystal packing conditions were revealed by analyzing the molecular and crystal structures

Structures 1–8

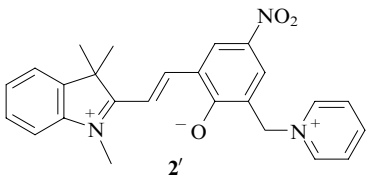


of different photochromic salts of spiro compounds with the aim of their application in the synthesis of hybrid photochromic para- and ferromagnets based on bimetallic tris(oxalates).

It was shown that, as opposed to neutral spiropyridopyran (SP) molecules, electrostatic interactions between the X^- anion and the quaternary N^+ atom in the crystals of their salt forms (SP^+X^-) hinder the packing of pyridopyran moieties in stacks (Fig. 3). The indoline moieties are arranged in stacks, whereas the pyridopyran moieties together with X^- anions are loosely packed between the stacks, thus enabling reversible photochromic transformations in the crystals. It was also found that the crystal packing of the salts in independent of the size of the X^- anion, but it is highly sensitive to substituents in the indoline moiety. It was demonstrated that the cationic building block, in which SP^+ exists in the closed form, can replace nonfunctional cations located between magnetic anion layers in bimetallic tris(oxalates).

By contrast, in crystals of halides, in which the cations are in the open [merocyanine (MC)] form (MC^+Cl^-), photochromic transformations were not observed under stationary irradiation. In the crystal structure of $MC^+Cl^- \cdot 3\,H_2O$ (MC^+ = **2′**, the open form of spiropyran **2** with R^1 = H, R^2 = NO_2), the MC^+ cations are planar and are arranged in closely packed translationally related stacks, while Cl^- anions and water molecules that form a hydrogen bond network are located in channels between the stacks (Fig. 4).

Structure 2′



The structure is additionally stabilized by electrostatic interactions between the indolium N^+ atom and the phenolate O^- atom (3.293 Å), as well as between the quaternary N^+ atom of the pyridinium moiety and the Cl^- anion (3.872 Å). This structure prevents the isomerization of the open form into the closed one under irradiation in solid state.

In the chromene cation, the C–O bond is also as elongated as in spiropyrans. However, photochromic transformations that take place in spiropyran salts are not

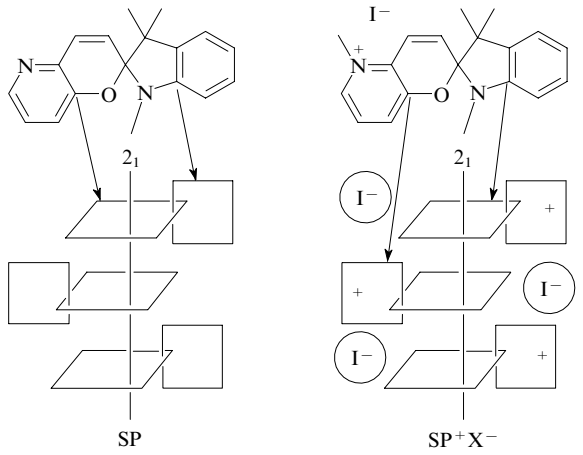


Figure 3. Schematic representation of the crystal packing of neutral spiropyran (SP) molecules of the indoline series and the related salt (SP^+X^-; X = I).[35]

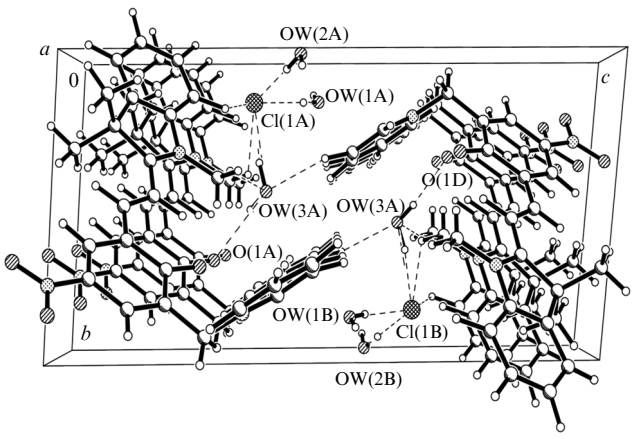


Figure 4. Schematic representation of the crystal packing of the salt $MC^+Cl^- \cdot 3\,H_2O$ (MC^+ = **2′**).[11]

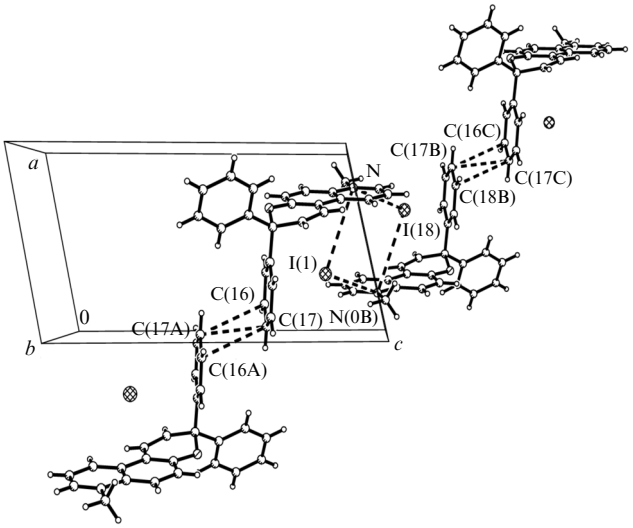


Figure 5. Fragment of the crystal structure of the chromene salt (Chr^+ = **4**, X = I).[35]
The moieties involved in van der Waals and ionic interactions are connected by dashed lines.

observed for chromene cations either in solid state or in solution. The crystal structure of chromene iodide Chr^+I^- (Chr^+ = **4**) is shown in Fig. 5. It can be seen that the organic cations are packed in blocks, and the I^- anions are located in channels.[35]

The chromene cations form columns along the *b* axis of the unit cell. The distance between the cations is 9.504(2) Å. This could provide the favourable conditions for photochemical transformations. However, in each cation the phenyl substituent forms shortened contacts with the corresponding ring in the cation from the adjacent column, which limits the possibility of moving this part of the cation during its rearrangement.[35] The pyran moiety of each cation is involved in Coulomb interactions with two I^- anions, and each anion is involved in electrostatic interactions with the pyran moiety of the cation from the adjacent column. This results in the formation of associates in the crystal structure. Assuming that the absence of photochromic transformations is associated only with the crystal structure of this compound, the revealed features of this structure can be considered as responsible for the impossibility of the existence of the open form of chromene in solid state.

The isomerization of iodides of chromene and quinoline spiropyran from the closed to the open form in the ground state was compared by quantum chemical methods[35] with full geometry optimization of both forms of these compounds at the B3LYP/6-31G level of theory using the GAUSSIAN-03 program.[35] According to the results of calculations, the closed form of chromene iodide is thermodynamically more stable. The total energy of this form is $\sim$3.2 kcal mol^{-1} lower than that of the open form. For quinoline spiropyran **3** (R = Me), the situation is opposite. Thus, the open form is thermodynamically more stable; the total energy of this form is $\sim$4.1 kcal mol^{-1} lower than that of the closed form.

Photochromic diarylethenes and their salt forms are of considerable interest in practical applications. For instance, 2,3-diarylcyclopenten-2-en-1-ones and their salt forms, which are representatives of a new family of photochromic diarylethenes, were recently synthesized, and their spectroscopic properties were studied in detail; these compounds have considerable potential for improvement of the functioning of photochromic molecules as molecular switches.[36, 37]

The photochromic ring closure in diarylethene **8** [Het is pyridine (Py)] was studied by femtosecond laser spectroscopy.[38] The absorption spectra of intermediate excited states were recorded in a broad delay time range (up to 500 ps). It was found that the characteristic time of transition from the initial electron-excited state to an intermediate state is $\sim$180 fs. The kinetics of this transition is characterized by a coherent wave packet with an oscillation period of $\sim$80 fs, which is quenched within $\sim$200 fs. The kinetic scheme was proposed for transitions from the initial excited state to the final product — a closed-ring isomer. Considerable changes in the intermediate spectra were observed on the time scale from 2 to 500 ps. It was hypothesized that these picosecond processes are controlled by conformational transitions.

It should be noted that diarylethene salts were not as yet isolated as single crystals. In our opinion, synthetic chemists should focus their efforts on the preparation of such systems. An analysis of the data published in the literature on the synthesis of diarylethene salts in a polycrystalline state and their physicochemical characteristics in solution and solid state suggests that these salts can serve as more efficient building blocks in the design of photomagnetic systems compared to photochromic salts with cations of the spirocyclic series. These salts may by of practical interest as a photochromic sublattice in molecule-based magnets for the construction of photochromic optical switches having high thermal and photochemical stability and, which is particularly interesting, as media for the development of superfast switching devices.

III. Synthesis, structures and properties of para- and ferromagnetic crystals with photochromic cations of the spirocyclic series

Although quite a few salts (mainly, mineral acid salts) of organic photochromes were synthesized in the past years, there is a limited number of hybrid structures based on these compounds.

Photochromic oxalate ferromagnetic materials were synthesized in two steps, with the first step being the preparation of intermediate photochromic paramagnetic tris(oxalates) of the appropriate 3d metal (M^1 in Scheme 1), generally Cr^{III} or Fe^{III}. The structures and properties of these compounds are also of interest and were studied in detail.

Scheme 1

$$SP^+X^- \xrightarrow{[M^{1(III)}(ox)_3]^{3-}} (SP^+)_3[M^{1(III)}(ox)_3]^{3-} \xrightarrow{M^{2(II)}Cl_2} \longrightarrow (SP^+)[M^{1(III)}M^{2(II)}(ox)_3]^-$$

For instance, the structural data for the oxalatochromate salt — 1-isopropyl-3,3,5′,6′-tetramethylspiro[indoline-2,2′-[2*H*]pyrano[3,2-*b*]pyridinium] tris(oxalato)chromate(III) {see Scheme 1, SP^+ = **1** (R = Me), $(SP^+)_3[Cr(ox)_3]^{3-}$} — were obtained.[39]

The crystal structure of this anhydrous salt is composed of the structural units $[3\,SP^+\cdots Cr(ox)_3^{3-}]$, in which the

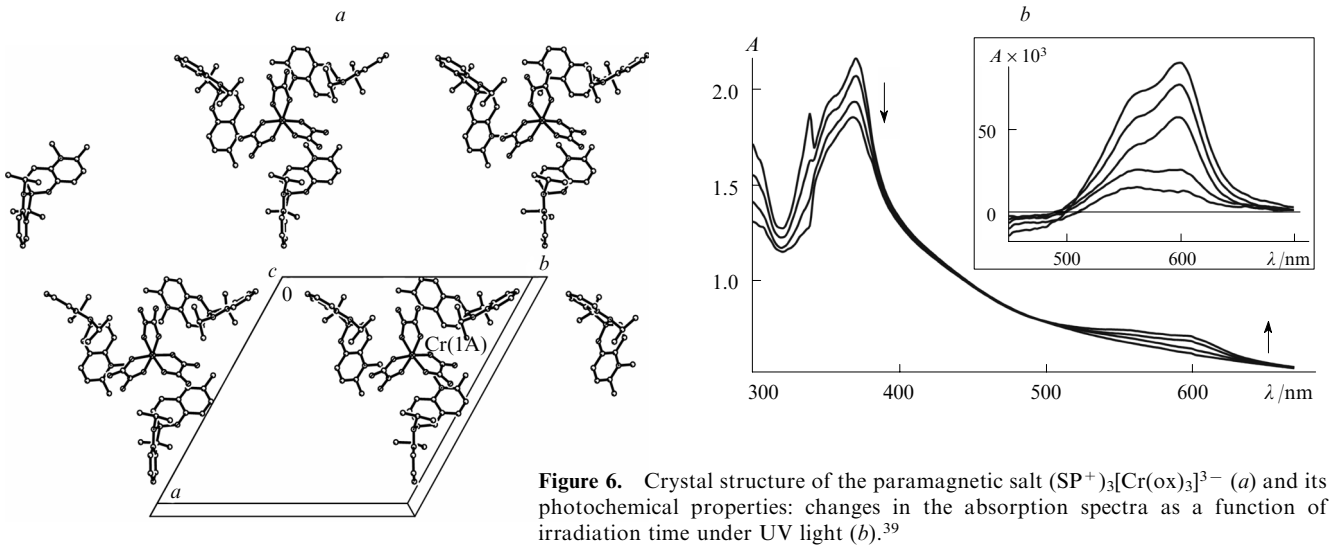
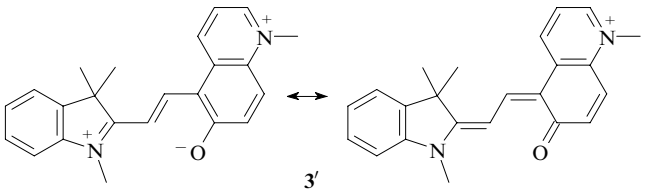


Figure 6. Crystal structure of the paramagnetic salt $(SP^+)_3[Cr(ox)_3]^{3-}$ (*a*) and its photochemical properties: changes in the absorption spectra as a function of irradiation time under UV light (*b*).[39]
The inset shows the difference absorption spectra under UV light irradiation.

spiropyran molecules are in the closed SP^+ form, the positively charged pyridopyran moieties pointing towards the oxalate groups, whereas the indoline moieties pointing towards the voids between the structural units. This structure (Fig. 6 *a*) proved to be favourable for photochromic transformations in crystals. Like in the salt SP^+X^-, fast reversible photochromic transformations occur in the crystals of $(SP^+)_3[Cr(ox)_3]^{3-}$. These transformations involve the generation of the MC^+ form (λ_{max} = 574 and 603 nm) under UV irradiation and the reverse cyclization under visible light irradiation. The irradiated crystals exhibit a slow colour fading in the dark (see Fig. 6 *b*).

The authors of this review synthesized for the first time single crystals of spiro[1,3,3,7′-tetramethylindolino-2,3′-3*H*-pyrano[3,2-*f*]quinolinium] tris(oxalato)chromate(III) [see Scheme 1, SP^+ = **3** (R = Me)],[40] in which the cation exists in the open MC^+ form **3′** (Scheme 2), $(MC^+)_3[Cr(ox)_3]^{3-} \cdot 13\,H_2O$, although it is in the closed (SP^+) form in the starting iodide.[34] It was found that the MC^+ cations in the cation layer of the complex are parallel to each other and form a close packing, and the anion layer is composed of oxalatochromate anions and water molecules linked together by hydrogen bonds (Fig. 7). This compound does not exhibit photochromic properties characteristic of salts of cationic spiropyrans since spiropyrans loss photochemical activity in this packing.

Scheme 2



3′

The SQUID (Superconducting Quantum Interference Device) magnetometry showed that the paramagnetic tris(oxalato)chromate anions exist as a mixture of states with spins $S = 1$ and $S = 3/2$. It should be noted that the anions in the $(SP^+)_3[Cr(ox)_3]^{3-}$ structure containing the cation in the closed SP^+ form are in the $S = 1$ state,[39] whereas the anions in the $(MC^+)_3[Cr(ox)_3]^{3-} \cdot 13\,H_2O$ structure containing the cation in the open MC^+ form exist predominantly in the $S = 3/2$ state.[40] The UV irradiation of both salts is accompanied by an irreversible change in exchange interactions and the average spin value. In the salt with the MC^+ cation, the average spin decreases from the initial value 3/2 to 1 (the average spin increases from 1 to 3/2 in the salt with the SP^+ cation), and a crossover from antiferromagnetic to ferromagnetic exchange correlations is observed (*vice versa* in the salt with the SP^+ cation). This is evidence that the structures of the salt and the isomeric form of the cation have a substantial effect on the magnetic properties of the compound.

The paramagnetic compounds with the $[M^{III}(ox)_3]^{3-}$ anion, where M = Cr^{3+}, Mn^{3+}, Fe^{3+}, Co^{3+}, were isolated in the solid state. These compounds contain spiro cation SP^+ **2** ($R^1 = R^2$ = H), which does not exhibit photochromism in the solid state. As opposed to the salts studied earlier, bromide of this spiropyran does not form a crystal structure favourable for photochromic transformations. The benzopyran moieties responsible for photochromic transforma-

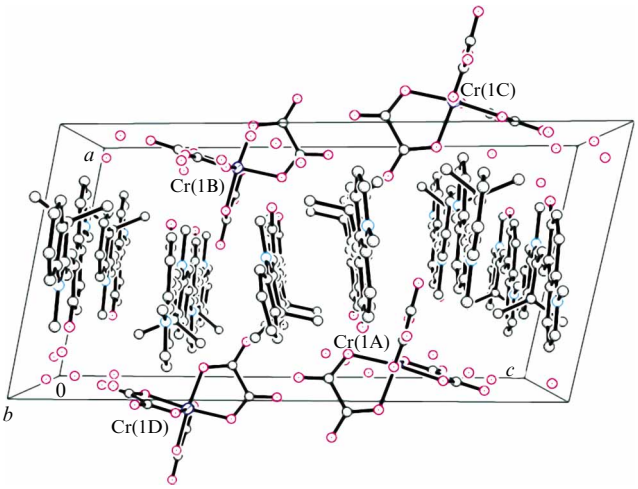


Figure 7. Crystal structure of the salt $(MC^+)_3[Cr(ox)_3]^{3-} \cdot 13\,H_2O$ (MC^+ = **3′**).[40]

tions are located in the loosely packed part of the structure. The SP^+ cations in the structural blocks are closely packed. The Br^- ions and water molecules are located between the stacks and are involved in a hydrogen bond system. There are also pyridinium moieties in the space between the stacks. The $N^+\cdots Br^-$ distance is 3.57 Å (Fig. 8).[41]

In all tris(oxalate) complexes with this spiro cation, no changes in the magnetic moment (M) were observed under UV irradiation (except for the complex with $M = Fe^{3+}$ after its irradiation for 5 h). The average value of the spin (5/2) and a 2% decrease in the amount of magnetic species under irradiation were determined from the approximation of the magnetic field dependence of the magnetic moment of the sample by the Brillouin function. The magnetic moment hysteresis before and after irradiation was absent. Apparently, a decrease in the magnetic moment of the sample with Fe^{3+} observed under UV irradiation is attributed to the side reduction of Fe^{3+} to Fe^{2+}.

Paramagnetic Mn^{3+} complexes have the d^4 configuration with $S = 2$. Their ESR spectra show a characteristic single asymmetric line ($g = 2.0046$). The double integration of the ESR spectra provided an estimate of the magnetic susceptibility (χ). An analysis of the plots of χT *versus* T compared with that for $K_3Mn(ox)_3 \cdot 3H_2O$ demonstrated that the replacement of the inorganic cation in the starting compound with the organic SP^+ cation results in a crossover from antiferromagnetic to ferromagnetic correlations in the complex $(SP^+)_3[Mn(ox)_3]^{3-} \cdot 4H_2O$.

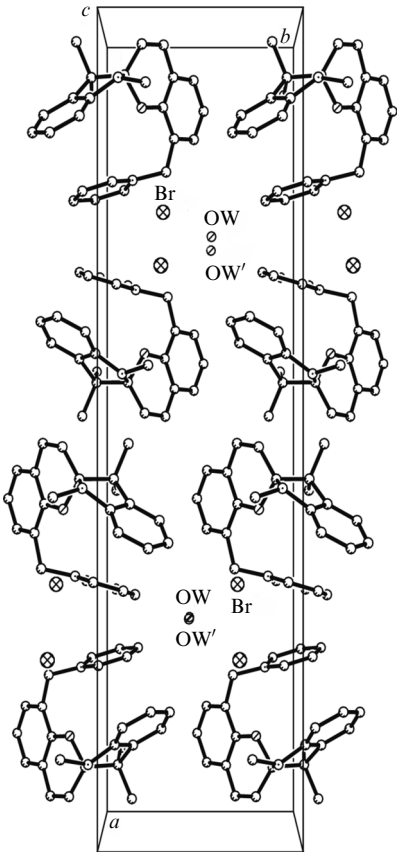


Figure 8. Fragment of the crystal packing of the nonphotochromic spiropyran salt $SP^+Br^- \cdot H_2O$ (SP^+ = **2**; $R^1 = R^2 = H$).[41]

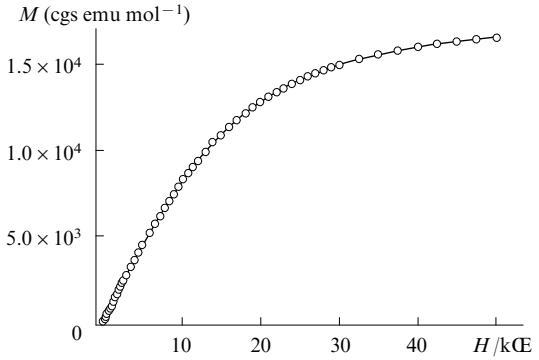


Figure 9. Dependence of the magnetic moment (M) of the complex $(Chr^+)_3[Cr(ox)_3]^{3-} \cdot 3H_2O$ (Chr^+ = **4**) on the external magnetic field strength at 2 K.[35]
The solid line represents the approximation by the Brillouin function with spin $S = 3/2$.

Tris(oxalato)chromate(III) with the chromene cation **4** also exhibits paramagnetic behaviour (Fig. 9). At 2–5 K, the effective magnetic moment is 3.89 μ_B. This value is almost equal to the theoretical value $\mu_{eff} = g[S(S + 1)]^{1/2} = 3.87$ μ_B calculated for noninteracting spins of Cr^{3+} ions. The fact that only Cr^{3+} ions contribute to the magnetic properties at 2 K is also evidenced by the approximation of the field dependence of the magnetic moment by the Brillouin function, according to which the

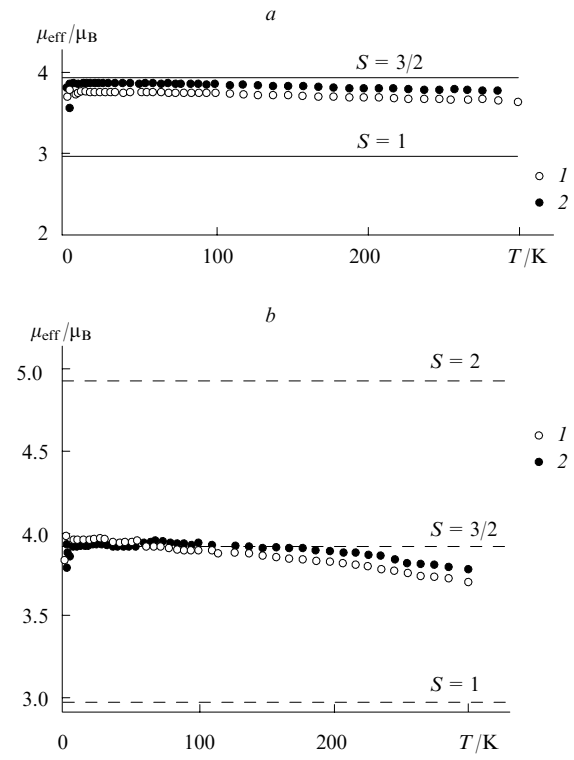


Figure 10. Temperature dependence of the effective magnetic moment of the complexes $(DAE^+)_3[Cr(ox)_3]^{3-} \cdot 3H_2O$ in a stationary magnetic field $H = 1000$ Oe before (*1*) and after (*2*) UV irradiation.
(*a*) DAE^+ = **7** (Het = Py) (*b*) DAE^+ = **8** (Het = Py) (authors' data presented at the conference[42]).

average spin is 3/2, *i.e.*, this spin is equal to the spin of Cr^{3+} ions.

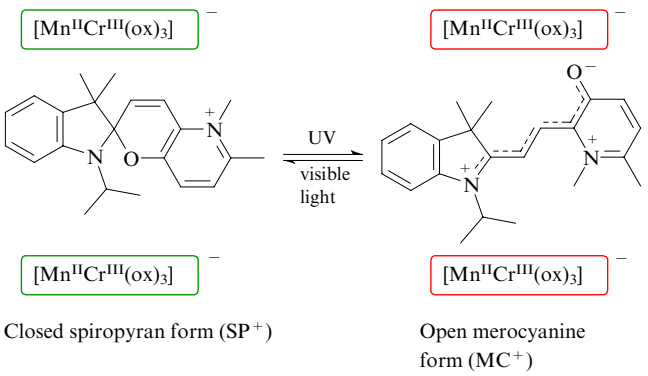
A similar situation was observed for tris(oxalato)chromates(III) with different diarylethene cations DAE^+ (Fig. 10).

Therefore, we developed approaches to the synthesis of new functional structural blocks, such as photochromic paramagnetic 3d metal tris(oxalates), and performed spectroscopic-kinetic and magnetometric studies aimed at the use of these compounds for the design of bimetallic photoactive ferromagnetic systems (crystals, nanostructures and polymer composites).

Numerous attempts to synthesize single crystals of ferromagnets with photochromic organic cations have failed.

Bénard *et al.*[24, 43, 44] were the first to synthesize powders of ferromagnetic tris(oxalates) with photochromic spiropyrans by the interacalation of photochromes into the magnetic lattice of bimetallic tris(oxalates) (Scheme 3).

Scheme 3



Closed spiropyran form (SP^+)

Open merocyanine form (MC^+)

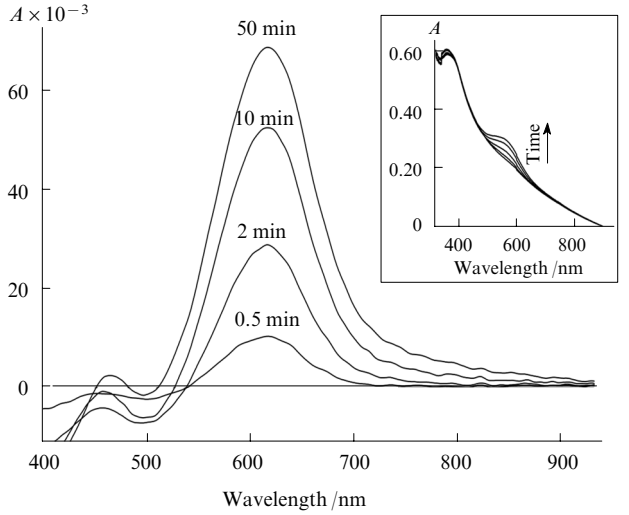


Figure 11. Reversible photochromic transformations of the bifunctional system $SP^+[Cr^{III}Mn^{II}(ox)_3]^-$ (SP^+ = **2**; R^1 = Cl, $R^2 = NO_2$) before and after irradiation with UV light (337 nm). The irradiation was performed at 298 K.[46]
The inset shows the changes in the electronic absorption spectra of the polycrystalline sample under visible light irradiation.

Under UV light irradiation, the initial spiropyran (SP^+) form is transformed into the merocyanine form (MC^+), whereas the visible light irradiation induces the reverse process. The open MC^+ form in the iodide SP^+I^- is thermodynamically unstable and relaxes to the initial state, whereas both forms proved to be stable in the hybrid compound. Apparently, interactions between the anion layer and the organic cation increase the energy barrier between the SP^+ and MC^+ forms. At T_C = 5.5 K, the complex undergoes a transition to a ferromagnetic state. Although the transition temperature remains the same, a considerable change in the shape of the magnetic hysteresis loop is observed after UV light irradiation (355 nm), which causes the transformation of the initially soft magnet into the hard magnetic state. This process is irreversible and is

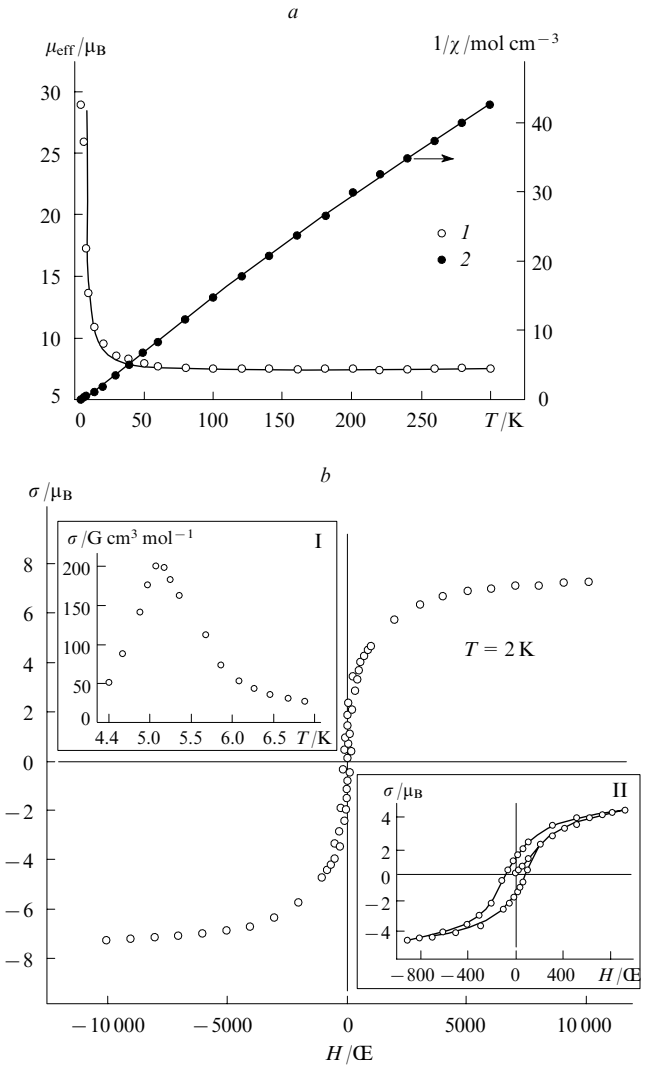


Figure 12. (*a*) Temperature dependences of the effective magnetic moment (*1*) and the inverse magnetic susceptibility (*2*) for $(SP^+)[CrMn(ox)_3]^-$ (SP^+ = **2**; R^1 = H, $R^2 = NO_2$) in the range of 5–300 K; (*b*) the field dependence of the magnetization of $(SP^+)[CrMn(ox)_3]^-$ at 2K.[45]
The insets show the dependence $\sigma(T)$ in a weak magnetic field (I) and the hysteresis loop (II).

attributed to the formation of structural defects in the anion lattice caused by the isomerization of the cation.

Polycrystalline ferromagnets with photochromic cations SP^+ = **2** (R^1 = H, Cl; $R^2 = NO_2$) have been synthesized and characterized.[45,46] The reaction mixture was continuously irradiated with light at $\lambda > 500$ nm in order to shift the equilibrium between two forms in polar solvents towards the closed form. The resulting salts with the bimetallic tris(oxalate) anions $[Cr^{III}\ Mn^{II}(ox)_3]^-$, like halides of the starting spiropyrans, exhibit reversible photochromic properties in the solid state (Fig. 11). It should be noted that these changes are apparently associated with reactions on the surface. Both forms are present in the samples under study before irradiation and undergo interconversions under UV irradiation. The rate at which the equilibrium is achieved in the dark is negligible ($k = 10^{-6} - 10^{-7}$ s^{-1}).

Both compounds are ferromagnets with $T_C \approx 5$ K (Fig. 12). The value of μ_{eff} at 300 K ($\sim 7\ \mu_B$) is in good agreement with the value calculated for weakly interacting Mn^{II} and Cr^{III} ions (7.07 μ_B, $g = 2$). The field dependence of the magnetization at 2 K shows a hysteresis (see Fig. 12*b*, inset II). The saturation of the magnetization is achieved at $\sim 10\,000$ Œ and is 6.8 – 7.0 μ_B. This saturation is lower than the value expected for the eight-spin configuration of $Cr^{III}Mn^{II}$ (3 + 5 = 8). The coercive force in the compounds varies from 30 to 80 Œ and apparently depends on their crystal structure. However, as opposed to photochromic magnets,[41] there is no significant influence of photochromic transformations of SP^+ **2** (R^1 = H, Cl; $R^2 = NO_2$) on the rigidity of the magnetic sublattice in these compounds. Apparently, this is attributed to the fact that spirocyclic pyridopyrans **1** (R = Me) contain the quaternary N^+ atom in the π-conjugated part of SP^+ responsible for photochromic transformations, whereas the N^+ atom in benzopyran cations **2** is located in the side chain of the substituent.

Therefore, crystalline hybrid structures were prepared for the first time from the specially synthesized salts of organic photochromes (spiropyrans, chromenes, dihetarylethenes) and magnetic networks [para- and ferromagnetic transition metal tris(oxalates)], and their properties in solid state, including under irradiation, were studied.

IV. Synthesis and properties of materials based on photochromic 3d metal tris(oxalates)

IV.1. Ordered nanostructures

The assembly of nanoobjects to a system of interacting elements, which can be controlled by external factors and which are compatible with the element basis of optoelectronic devices, is one of key fields in nanoindustry.[47] The design of powdered nanostructures has attracted considerable attention and begun to bear fruit. It was shown that the nanostructuring results in a substantial change in the physical properties of organic and metal-organic materials.[48,49] However, the actual application of nanosized multifunctional materials is possible if they are arranged in ordered structures. It should be noted that 3d metal complexes with photochromic cations offer the following advantages over known compounds possessing photocontrolled magnetism: 1) the magnetic moment can be reversibly changed at room temperature under light irradiation; 2) the magnetic moment is changed by a large amount

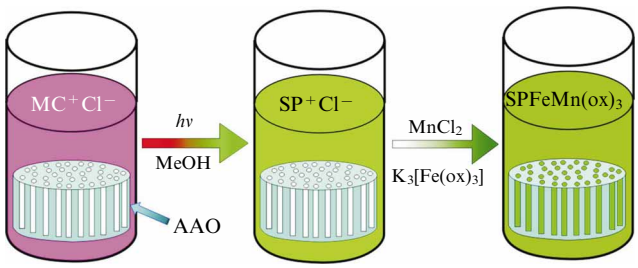


Figure 13. Scheme of the synthesis of micro- and nanocrystals of $(SP^+)[Fe^{III}Mn^{II}(ox)_3]^-$ (SP^+ = **2**; R^1 = H, $R^2 = NO_2$).[47]

(50% – 100%) under light irradiation; 3) these materials are convenient for nanostructuring — the construction of nanofilms, which can be considered as a technology project for the creation of nanochips with photocontrolled magnetic elements and other high-tech devices.

First results providing evidence that nanomatrices can be filled with photochromic spiropyran molecules were obtained earlier by researchers[50,51] who revealed some specific effects caused by nanostructuring (optically switchable luminescence, photocontrolled nanovalves that control the transport of solvent molecules through nanopores and photoswitching of electrical conductivity). All these results indicate that the nanostructuring of photomagnetic multifunctional compounds can also bring about new physical effects.

The compound $(SP^+)[Fe^{III}Mn^{II}(ox)_3]^-$ with photochromic cation **2** (R^1 = H, $R^2 = NO_2$) was used as a sample with the expected photomagnetic effect for the purpose of creating an array of nanostructures that meet the above-mentioned requirements. Nanocrystals were synthesized in an anodized aluminium oxide (AAO) membrane with a pore diameter of 20 nm under continuous UV irradiation (Fig. 13).

The magnetic properties of microcrystals were similar to those described previously. The temperature dependence of the product of the magnetic moment of the sample (M) and

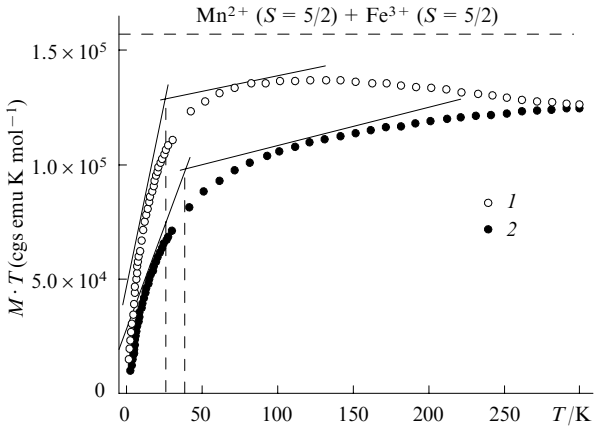


Figure 14. Temperature dependences of the product of the magnetic moment and the temperature ($M \cdot T$) for nano- (*1*) and microcrystals (*2*) of the compound $(SP^+)[Fe^{III}Mn^{II}(ox)_3]^-$ (SP^+ = **2**; R^1 = H, $R^2 = NO_2$).[47]
Measurements were performed in a field H = 20 kŒ.

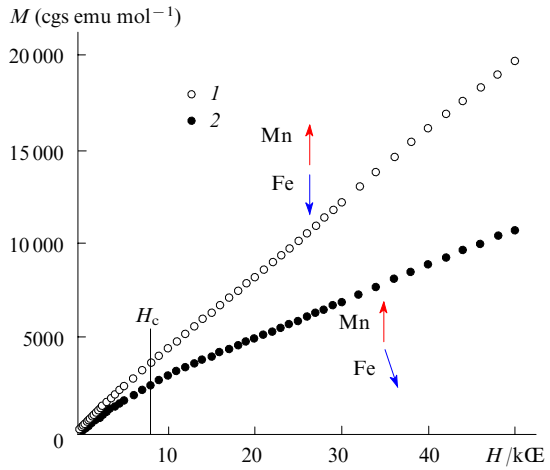


Figure 15. Plot of the magnetic moment (M) *versus* the external field (H) at 2 K in nanocrystals (*1*) and microcrystals (*2*) of the compound $(SP^+)[Fe^{III}Mn^{II}(ox)_3]^-$ (SP^+ = **2**; R^1 = H, $R^2 = NO_2$).[47]
The mutual orientation of the spins of the Fe^{3+} and Mn^{2+} ions in collinear and noncollinear antiferromagnets is indicated.

the temperature shows a transition to an antiferromagnetic state at 30–50 K (Fig. 14). The value of $M \cdot T$, which is proportional to the square of the effective magnetic moment, strongly deviates towards smaller values compared to a constant value that would be expected of a paramagnetic material. The existence of a long-range antiferromagnetic order is evidenced by the dependence of the magnetic moment of the sample (M) on the magnetic field (H) (Fig. 15). This plot has an inflection point at H_c = 8 kŒ characteristic of spin-flop transitions in noncollinear antiferromagnets. The shape of the plot $M(H)$ is substantially different from the Brillouin function expected for the paramagnetic state of the material. The inflection point in the plot $M(H)$ is a typical sign of a noncollinear (spin-canted) antiferromagnet, in which the Dzyaloshinskii–Moriya interaction gives rise to the magnetization perpendicular to two-dimensional oxalate networks.

The dependences $M \cdot T(T)$ and $M(H)$ for nanowires are essentially different (see Figs 14 and 15) from those for microcrystalline samples. The temperature dependence of $M \cdot T$ shows a smooth maximum at 70–100 K. The decay of $M \cdot T$, which attests to the transition to an antiferromagnetic state, occurs at lower temperatures ($\sim$ 20 K, see Fig. 14). The dependence of the magnetic moment of a nanostructured sample degenerates to a straight line (see Fig. 15) because the inflection point observed for a microcrystalline sample at H_c = 8 kŒ disappears. Since the transition from microcrystals to nanosized samples leads to a change in the magnetic properties, it can be suggested that the sizes of nanostructures were smaller than the characteristic lengths essential for a long-range magnetic order. This, in turn, can lead to the artificial assignment of the principal axis of the magnet along nanowires and to the suppression of the noncollinear component of the magnetization. Earlier, it was demonstrated [52, 53] that two phases with a collinear and noncollinear spin order coexist in two-dimensional networks of iron and manganese oxalates. Apparently, the limitation of the nanowire diameter in our experiments results in the preferential growth of the collinear phase and the suppression of the phase exhibiting noncollinearity. This is evidenced by the absence of an inflection point in the plot of the magnetic moment *versus* the field (see Fig. 15). Besides, this point of view is supported by a sharper temperature transition to an antiferromagnetic state near 30 K in nanocrystals compared with the diffuse transition in microcrystals associated with the coexistence of two phases (see Fig. 14).

Therefore, the effors led to the fabriaction of the previously unavailable ordered arrays of nanowires of photochromic antiferromagnetic materials based on 3d metal tris(oxalates) and spiropyrans of the indoline series, which are incorporated into pores of anodized aluminium oxide with a diameter of 20 nm. A change in the magnetic properties of the resulting materials due to their nanostructuring was observed. It was demonstrated that the nanostructuring leads to the suppression of a noncollinear spin ordering, thus transforming a noncollinear antiferromagnet into a uniaxial antiferromagnet.

IV.2. Polymer composites

In recent years, the construction of photochromic polymer materials has attracted considerable attention.[50, 54, 55] The methodology developed by the authors of this review for the synthesis of photochromic polymer magnetic compositions relies on the incorporation of photochromic metal-organic compounds into a polymer matrix, as well as on the control and modification of their properties in order to achieve synergistic effects.

As shown above, various photomagnetic effects are observed in crystals of photochromic magnets. These effects are associated with the light effect on the coercive force,[43, 56, 57] the electron redistribution between the organic photochromic and inorganic magnetic subsystems [58] and so on.

Homogeneous polyvinylpyrrolidone (PVP) composites incorporating paramagnetic 3d metal tris(oxalate) complexes with photochromic spiropyran of the indoline series **3** (R = Me) bearing a quinoline moiety were synthesized for the first time. The photochemical characteristics and magnetic properties of these compounds were studied by SQUID magnetometry. The ESR spectra were found to be changed under UV irradiation in polymer PVP films incorporating a photochromic paramagnet.[59]

Specially synthesized highly branched polystyrene was also used as a polymer matrix. This polymer simultaneously stabilizes a 10 mass % suspension of particles of the photochromic ferromagnetic material $(SP^+)[Cr^{III}Mn^{II}(ox)_3]^- \cdot H_2O$ (SP^+ = **1**, R = Me) (authors' data presented at the conference).[60] A suspension of a ferromagnetic powder in a toluene solution of polystyrene was sonicated and placed onto a fluoroplastic substrate with a specified geometry, the solvent was removed and the films were kept at 40 °C to a constant weight. A micrograph of the composite is shown in Fig. 16 *a*. It can be seen that ferromagnetic particles are uniformly distributed in the film. However, inclusions of large particles are observed despite the fact that the ferromagnetic powder has been preliminary ground.

The micrographs and results of energy-dispersive X-ray spectral (EDX) analysis (see Fig. 16 *b*) of polystyrene films containing a photochromic ferromagnetic material confirm the presence of elongated particles at a high accelerating voltage (14 kV) and a depth of penetration of 4–6 μm. The

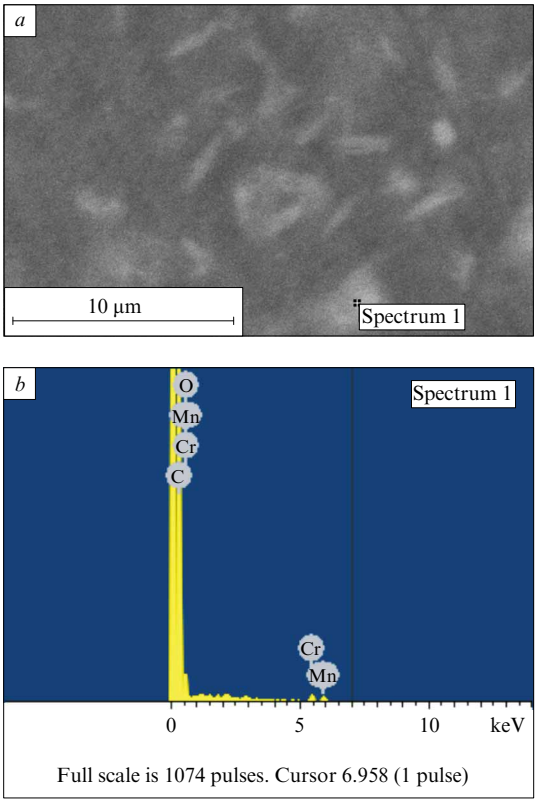


Figure 16. Micrograph (*a*) and results of energy-dispersive X-ray spectral analysis (*b*) of the polymer composite with the ferromagnetic material $(SP^+)[Cr^{III}Mn^{II}(ox)_3]^- \cdot H_2O$ (SP^+ = **1**, R = Me).[60]

particle size was 0.5–2 μm in length and up to 0.5–0.6 μm in width.[60]

The energy-dispersive X-ray spectral analysis, studies of the photochemical activity of the synthesized polymer composite and investigations of its magnetic characteristics in a wide temperature range by SQUID magnetometry (Figs. 17–20) (authors' data presented at the conference) [61]

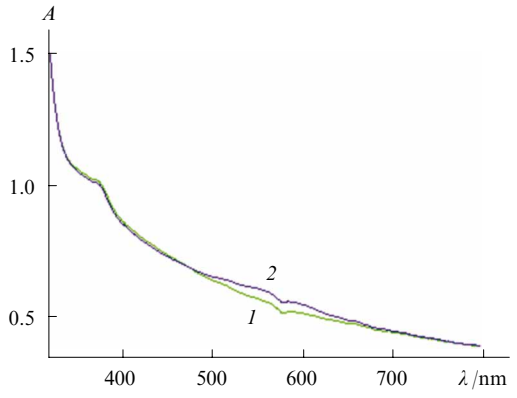


Figure 17. Absorption spectra of a highly branched polystyrene composite containing 10 mass % of particles of the photochromic ferromagnetic material $(SP^+)[Cr^{III}Mn^{II}(ox)_3]^- \cdot H_2O$ with the photochromic cation SP^+ = **1** (R = Me) before (*1*) and after (*2*) UV light irradiation (355 nm) for 2 min.[60]
The absorption maximum of the coloured form is 564 nm.

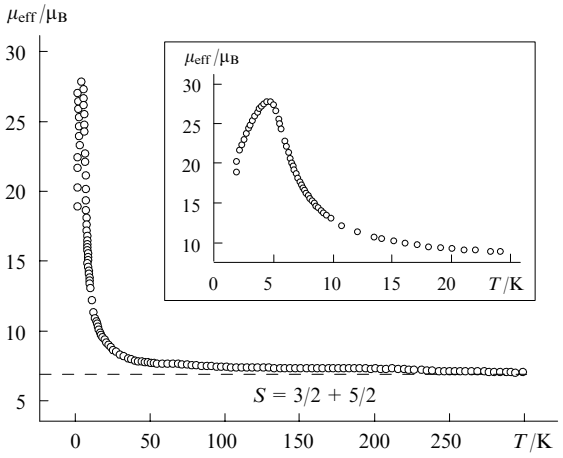


Figure 18. Temperature dependence of the effective magnetic moment of a highly branched polystyrene composite containing 10 mass % of particles of the photochromic ferromagnetic material $(SP^+)[Cr^{III}Mn^{II}(ox)_3]^- \cdot H_2O$ (SP^+ = **1**, R = Me).[61]
The inset shows the 2–25 K range of the plot on an enlarged scale.

demonstrated that homogeneous polymer composites of highly branched polystyrene incorporating particles of a photochromic ferromagnetic material exhibit properties of the starting crystalline sample of the complex.

The resulting composite of highly branched polystyrene containing 10 mass % of particles of the photochromic ferromagnetic material $(SP^+)[Cr^{III}Mn^{II}(ox)_3]^- \cdot H_2O$ with the photochromic cation SP^+ = **1** (R = Me) displays photochromic properties characteristic of spiropyran salts.[32, 38, 60] Under UV irradiation, the equilibrium is shifted towards the open form, whereas the reverse process occurs under visible light irradiation. Figure 17 presents the absorption spectra of a polymer sample containing 10 mass % of the complex before and after UV irradiation. The spectra show an absorption band of the open form at 520–630 nm with a maximum at 564 nm, which is consistent with the spectroscopic characteristics of the coloured form of this cation in the iodide [62] and monometallic oxalatochromate.[36]

The temperature dependence of the effective magnetic moment of highly branched polystyrene containing 10 mass % of particles of the photochromic ferromagnetic material $(SP^+)[Cr^{III}Mn^{II}(ox)_3]^- \cdot H_2O$ (SP^+ = **1**, R = Me) is shown in Fig. 18. At temperatures >50 K, the effective magnetic moment is almost constant and is very close to the theoretical value of 7.09 μ_B for a system of noninteracting spins S_{Cr} = 3/2 and S_{Mn} = 5/2. An increase in the effective magnetic moment of the composite is observed as the temperature decreases below 50 K and it reaches the maximum value at T = 5 K.

The field dependence of the magnetic moment at T = 2 K is shown in Fig. 19. It can be seen that the plot for the composite reaches the saturation at fields >10 kŒ. At a saturation, the magnetic moment is 8 μ_B. However, the residual magnetization per structural unit of the complex is 2 μ_B. The high value of the residual magnetization is apparently attributed to the presence of large ferromagnetic inclusions in the sample. A wide size distribution of granules of the complex is one of the factors responsible for a complex shape of the hysteresis loop. Since the coercive

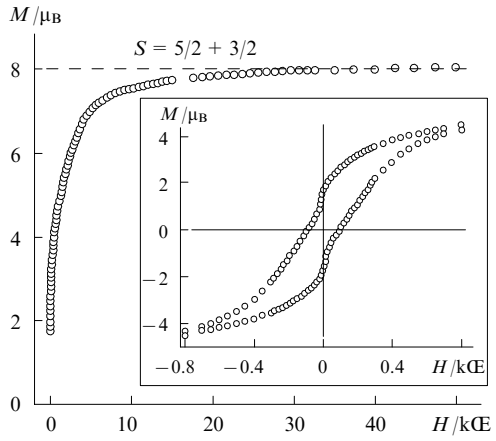


Figure 19. Field dependence of the magnetic moment of a highly branched polystyrene composite containing 10 mass % of particles of the photochromic ferromagnetic material $(SP^+)[Cr^{III}Mn^{II}(ox)_3]^- \cdot H_2O$ (SP^+ = **1**, R = Me) at $T = 2$ K.[61] The inset shows a hysteresis loop.

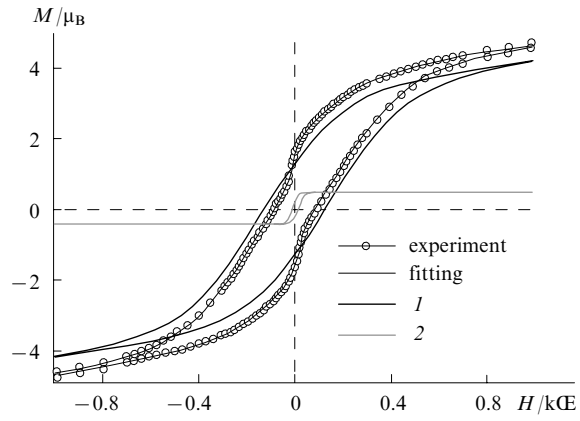


Figure 20. Magnetic hysteresis loop of a highly branched polystyrene composite containing 10 mass % of particles of the photochromic ferromagnetic material $(SP^+)[Cr^{III}Mn^{II}(ox)_3]^- \cdot H_2O$ (SP^+ = **1**, R = Me) at $T = 2$ K (empty points) and its decomposition (thin solid line) into the sum of two components *1* and *2*.[61]

force of an individual inclusion depends on its size, the presence of 'large' ferromagnetic inclusions among a large amount of 'small' dispersed particles results in an integrated character of the hysteresis loop of the magnetization of the sample. The decomposition of the magnetic hysteresis loop is shown in Fig. 20. The hysteresis loop with a smaller value of the coercive force corresponds to dispersed particles of the complex, whereas the magnetic hysteresis loop with larger coercive force corresponds to 'larger' ferromagnetic inclusions.

Therefore, the conditions were found for the fabrication of branched polystyrenes with a high percentage of a highly branched fraction having a low intrinsic viscosity. These conditions are suitable for the preparation of moderately viscous highly concentrated solutions of high-molecular-weight polystyrene. It was demonstrated that the use of highly branched polystyrene allows the preparation of time-stable dispersions of particles of 3d metal tris(oxalate) complexes and application of the latter for the formation of polymer films with a uniform particle distribution in the bulk. The properties of the first polymer composites of highly branched polystyrene and nanomaterials containing hybrid systems — molecule-based magnets with a photochromic sublattice — were investigated. This provides opportunities for applications of the above-described procedure for the insertion of other classes of molecule-based magnets, including single-molecule magnets, into a polymer (or inorganic nanosized) matrix with the aim of developing innovative materials for miniature high-density data storage molecular devices, as information media in quantum computers, spintronics and so on.

* * *

Photochromic compounds hold a key place in scientific research aimed at developing new functional materials, including light filters, molecular switches, chemosensors and 3D optical memory devices. Based on systematic studies of the structural features and properties of individual building blocks, such as photochromic and magnetic, it was shown that different cations of the spirocyclic series, as well as dihetarylethenes and anions of para- and ferromagnetic transition metal tris(oxalates), can be combined in the same crystal lattice. Such materials as hybrid photochromic materials, which were synthesized by the authors of this review and then structurally characterized by IR, UV and NMR spectroscopy and X-ray diffraction, were demonstrated to be convenient starting substances for the nanostructuring — the construction of nanofilms and nanowires as ordered ensembles of nanoelements.

We would like to thank our colleagues, who have participated in our research, the results of which are summarized in the present review. This review was written with the financial support of the Presidium of the Russian Academy of Sciences within the framework of the programme 'Fundamentals for Basic Research of Nanotechnology and Nanomaterials'.

References

1. H Dürr, T H Bouas-Lausrent *Photochromism: Molecules and Systems* (Revised Edn) (Amsterdam: Elsevier, 2003)
2. S Kawata, Y Kawata *Chem. Rev.* **100** 1777 (2000)
3. *Organic Photochromic and Thermochromic Compounds* (Eds J C Crano, R J Guglielmetti) (New York: Plenum, 1999)
4. M Irie *Chem. Rev.* **100** 1685 (2000)
5. M Irie, T Fukaminato, T Sasaki, N Tamai, T Kawai *Nature (London)* **420** 759 (2002)
6. *Molecular Switches* (Ed. B L Feringa) (Weinheim: Wiley-VCH, 2001)
7. Y Li, H Zhang, Ch Qi, X Guo *J. Mater. Chem.* **22** 4261 (2012)
8. L A Frolova, P A Troshin, D K Susarova, A V Kulikov, N A Sanina, S M Aldoshin *Chem. Commun.* **51** 6130 (2015)
9. V A Barachevsky *Rev. J. Chem.* **3** 52 (2013) [*Obzornyi Zh. Khim.* **3** 58 (2013)]
10. S M Aldoshin *J. Photochem. Photobiol., A* **200** 19 (2008)
11. S M Aldoshin *Russ. Chem. Bull., Int. Ed.* **57** 718 (2008) [*Izv. Akad. Nauk, Ser. Khim.* 704 (2008)]
12. *New Frontiers in Photochromism* (Eds M Irie, Y Yokoyama, T Seki) (Tokyo: Springer, 2013)
13. V I Ovcharenko, R Z Sagdeev *Russ. Chem. Rev.* **68** 345 (1999)

14. H Tamaki, Z J Zhong, N Matsumoto, S Kida, M Koikawa, N Achiwa, Y Hashimoto, H Okawa *J. Am. Chem. Soc.* **114** 6974 (1992)
15. H Tamaki, M Mitsumi, K Nakamura, N Matsumoto, S Kida, H Okawa, S Iijima *Chem. Lett.* 1975 (1992)
16. L O Atovmyan, G V Shilov, R N Lyubovskaya, E I Zhilyaeva, N S Ovanesyan, Yu G Morozov, S I Pirumova, I G Gusakovskaya *Pis'ma Zh. Eksp. Teor. Fiz.* **58** 818 (1993)
17. S Decurtins, H W Schmalle, H R Oswald, A Linden, J Ensling, P Gütlich, A Hauser *Inorg. Chim. Acta* **216** 65 (1994)
18. S G Carling, C Mathonière, P Day, K M Abdul Malik, S J Coles, M B Hursthouse *J. Chem. Soc., Dalton Trans.* 1839 (1996)
19. L O Atovmyan, G V Shilov, R N Lyubovskaya, E I Zhilyaeva, N S Ovanesyan, O A Bogdanova, S I Pirumova *Koord. Khim.* **23** 683 (1997)
20. G V Shilov, L O Atovmyan, N S Ovanesyan, A A Pyalling, L Bott'yan *Koord. Khim.* **24** 305 (1998)
21. M Clemente-León, E Coronado, J R Galán-Mascarós, C J Gómez-García *Chem. Commun.* 1727 (1997)
22. E Coronado, J R Galán-Mascarós, C J Gómez-García, V Laukhin *Nature (London)* **408** 447 (2000)
23. T G Prokhorova, L I Buravov, E B Yagubskii, L V Zorina, S V Simonov, R P Shibaeva, V N Zverev *Eur. J. Inorg. Chem.* 3933 (2014)
24. S Bénard, P Yu, J P Audière, E Rivière, R Clément, J Guilhem, L Tchertanov, K Nakatani *J. Am. Chem. Soc.* **122** 9444 (2000)
25. M Gruselle, Y Li, N Ovanesyan, V Makhaev, G Shilov, F Mushenok, C Train, S Aldoshin *Chirality* **25** 444 (2013)
26. Z K Nikitina, N S Ovanesyan, V D Makhaev, G V Shilov, S M Aldoshin *Dokl. Chem.* **437** 129 (2011) [*Dokl. Akad. Nauk* **437** 778 (2011)]
27. D V Korchagin, A N Utenyshev, K V Bozhenko, N A Sanina, S M Aldoshin *Russ. Chem. Bull., Int. Ed.* **60** 1040 (2011) [*Izv. Akad. Nauk, Ser. Khim.* 1016 (2011)]
28. *Licence to Use Agreement: Gaussian, Inc.* 340 Quinnipiac Street, Building 40, Wallingford, CT, 06492
29. K Yamaguchi, Y Takahara, T Fueno, in *Applied Quantum Chemistry* (Eds V H Smith Jr, H F Schaefer III, K Morokuma) (Dordrecht: Reidel, 1986) p. 155
30. S M Aldoshin, L A Nikonova, V A Smirnov, G V Shilov, N K Nagaeva *Russ. Chem. Bull., Int. Ed.* **54** 2113 (2005) [*Izv. Akad. Nauk, Ser. Khim.* 2050 (2005)]
31. S M Aldoshin, L A Nikonova, V A Smirnov, G V Shilov, N K Nagaeva *J. Mol. Struct.* **750** 158 (2005)
32. S M Aldoshin, L A Nikonova, G V Shilov, E A Bikanina, N K Artemova, V A Smirnov *J. Mol. Struct.* **794** 103 (2006)
33. N K Artemova, V A Smirnov, B G Rogachev, G V Shilov, S M Aldoshin *Russ. Chem. Bull., Int. Ed.* **55** 1605 (2006) [*Izv. Akad. Nauk, Ser. Khim.* 1548 (2006)]
34. V V Tkachev, S M Aldoshin, N A Sanina, B S Lukyanov, V I Minkin, A N Utenyshev, K N Khalanskiy, Yu S Alekseenko *Chem. Heterocycl. Compd.* **43** 576 (2007) [*Khim. Geterotsikl. Soedin.* 690 (2007)]
35. S M Aldoshin, N A Sanina, R B Morgunov, O A Fedorova, S V Paramonov, V B Lokshin, F B Mushenok, G V Shilov, K V Bozhenko, D V Korchagin *Russ. Chem. Bull., Int. Ed.* **59** 497 (2010) [*Izv. Akad. Nauk, Ser. Khim.* 487 (2010)]
36. V Z Shirinian, A A Shimkin, D V Lonshakov, A G Lvov, M M Krayushkin *J. Photochem. Photobiol. A* **233** 1 (2012)
37. A G Lvov, V Z Shirinian, A M Kavun, M M Krayushkin *Mendeleev Commun.* **24** 277 (2014)
38. S M Aldoshin, E A Yur'eva, N A Sanina, M M Krayushkin, D V Tsyganov, F E Gostev, I V Shelaev, O M Sarkisov, V A Nadtochenko *Russ. Chem. Bull., Int. Ed.* **60** 1118 (2011) [*Izv. Akad. Nauk, Ser. Khim.* 1093 (2011)]
39. S M Aldoshin, E A Yurieva, G V Shilov, L A Nikonova, V A Nadtochenko, E V Kurganova, R B Morgunov *Russ. Chem. Bull., Int. Ed.* **57** 2592 (2008) [*Izv. Akad. Nauk, Ser. Khim.* 2541 (2008)]
40. S M Aldoshin, N A Sanina, E A Yurieva, G V Shilov, E V Kurganova, R B Morgunov, B S Luk'yanov, V I Minkin *Russ. Chem. Bull., Int. Ed.* **57** 2495 (2008) [*Izv. Akad. Nauk, Ser. Khim.* 2445 (2008)]
41. N A Sanina, S M Aldoshin, G V Shilov, E V Kurganova, E A Yurieva, N A Voloshin, V I Minkin, V A Nadtochenko, R B Morgunov *Russ. Chem. Bull., Int. Ed.* **57** 1451 (2008) [*Izv. Akad. Nauk, Ser. Khim.* 1424 (2008)]
42. S M Aldoshin, R B Morgunov, N A Sanina, in *JSPS – CNRS Seminar 'New Horizons of Photochromism — from Design of Molecules to Applications' Arras, France, 2008* p. 32
43. S Bénard, P Yu *Adv. Mater.* **12** 48 (2000)
44. S Bénard, E Rivière, P Yu, K Nakatani, J F Delouis *Chem. Mater.* **13** 159 (2001)
45. S M Aldoshin, N A Sanina, V I Minkin, N A Voloshin, V N Ikorskii, V I Ovcharenko, V A Smirnov, N K Nagaeva *J. Mol. Struct.* **826** 69 (2007)
46. S M Aldoshin, N A Sanina, V A Nadtochenko, E A Yur'eva, V I Minkin, N A Voloshin, V N Ikorskii, V I Ovcharenko *Russ. Chem. Bull., Int. Ed.* **56** 1095 (2007) [*Izv. Akad. Nauk, Ser. Khim.* 1055 (2007)]
47. Patent RF 2445256 (2012)
48. *Physics, Chemistry and Application of Nanostructures* (Eds V E Borisenko, S V Gaponenko, V S Gurin) (Singapore: World Scientific, 2001)
49. *Organic Nanostructures* (Eds J L Atwood, J W Steed) (Weinheim: Wiley-VCH, 2008)
50. M-Q Zhu, L Zhu, J J Han, W Wu, J K Hurst, A D Q Li *J. Am. Chem. Soc.* **128** 4303 (2006)
51. I Vlassiouk, C-D Park, S A Vail, D Gust, S Smirnov *Nano Lett.* **6** 1013 (2006)
52. E Coronado, J-R Galán-Mascarós, C-J Gómez-García, J Ensling, P Gütlich *Chem. – Eur. J.* **6** 552 (2000)
53. N S Ovanesyan, V D Makhaev, S M Aldoshin, P Gredin, K Boubekeur, C Train, M Gruselle *Dalton Trans.* 3101 (2005)
54. A Spangenberg, R Métivier, J Gonzalez, K Nakatani, P Yu, M Giraund, A Léaustic, R Guillot, T Uwada, T Asahi *Adv. Mater.* **21** 309 (2009)
55. R Métivier, S Badré, R Méallet-Renault, P Yu, R B Pansu, K Nakatani *J. Phys. Chem. C* **113** 11916 (2009).
56. R B Morgunov, F B Mushenok, S M Aldoshin, N A Sanina, E A Yur'eva, G V Shilov, V V Tkachev *New J. Chem.* **33** 1374 (2009)
57. R B Morgunov, F B Mushenok, S M Aldoshin, E A Yur'eva, G V Shilov *Fiz. Tv. Tela* **51** 1568 (2009)
58. R B Morgunov, F B Mushenok, S M Aldoshin, N A Sanina *Zh. Eksp. Teor. Fiz.* **136** 775 (2009)
59. N A Sanina, V P Grachev, A I Dmitriev, R B Morgunov, O V Koplak, E A Yur'eva, D V Anokhin, D A Ivanov, S M Aldoshin *Russ. Chem. Bull., Int. Ed.* **62** 554 (2013) [*Izv. Akad. Nauk, Ser. Khim.* 552 (2013)]
60. N A Sanina, in *Book of Abstracts of 16th Annual Conference YUCOMAT 2014, Herceg Novi, Montenegro, 2014* p. 32
61. N A Sanina, in *Proceedings of 14th International Symposium on Functionally Graded Materials: Multiscale and Multifunctional Structures, Bayreuth, Germany, 2016* p. 54
62. E A Yurieva, S M Aldoshin, L A Nikonova, G V Shilov, V A Nadtochenko *Russ. Chem. Bull., Int. Ed.* **60** 1401 (2011) [*Izv. Akad. Nauk, Ser. Khim.* 1379 (2011)]